Adsorption strains in porous silicon

G. Dolino, D. Bellet, and C. Faivre

Laboratoire de Spectrométrie Physique, Université J. Fourier Grenoble I–CNRS (UMR 5588), Boîte Postale 87,
38402 Saint-Martin-d'Hères Cedex, France

X-ray-diffraction observations of strains induced by vapor adsorption are reported for porous silicon single-crystal samples. Two types of porous silicon (p and p^+) with very different pore structure are investigated. A low-pressure contraction is observed in p-type samples with spherical pores of about 3-nm diameter. In p^+-type samples, where the pores are cylindrical with a larger diameter of about 10 nm, a minimum of the lattice parameter versus the vapor pressure is observed when capillary condensation occurs with a distinct hysteresis between increasing and decreasing vapor pressure. Finally, an expansion is observed for complete wetting. These results are discussed for the different pressure ranges in relation to previous experimental and theoretical studies on adsorption strains. The analogous features observed for very different materials could have a common origin. The expansion is easily explained by the decrease of surface energy due to adsorption and wetting. It appears that the low-pressure contraction is partially related to the attractive van der Waals interactions induced by vapor adsorption in nanometer-size cavities. The softening of the elastic constants observed in porous silicon is discussed in order to explain the magnitude of the observed strains. [S0163-1829(96)01548-2]

I. INTRODUCTION

Fluid-solid interfacial phenomena, which have been studied for a long time, are always the subject of much interest.[1] Although vapor adsorption is always the standard characterization technique for porous materials,[2] some interesting questions remain unsolved.[3] Another active research field deals with intermolecular forces, which can be investigated with a surface force apparatus.[4] Adsorption and wetting phenomena are due to the action of molecular interactions between a fluid and an adsorbent, which usually is considered to be rigid. However, it is clear that the adsorbent is also submitted to the action of the molecular forces, and that some substrate deformation must exist, as indeed revealed by numerous observations of adsorption strains. The first report of these effects in a solid material is usually attributed to Meehan in 1927, for the adsorption of CO_2 in charcoal;[5] in the following years many observations of adsorption strains were reported, in particular by the Bangham group, also in charcoal,[6] and by Yates in porous silica.[7] These classical results were reviewed by Yates[7] in 1960, and by Sereda and Feldman[8] in 1967. Since that time, few new results on adsorption strains have been published: on the experimental side, we can mention the work of Dash *et al.*[9] on vapor adsorption in graphite, and of Thibault, Préjean, and Puech[10] on He adsorption in silica aerogel; there were also some related works on strain measurements in porous media during water freezing[11] or gel drying.[12] On the theoretical side, we can mention studies by Ericksson[13] and Ash, Everett, and Radke,[14] which will be developed below as a starting point for the discussion of our experimental results.

In this paper, we report measurements of adsorption strains in porous silicon (PS), a material which, after the recent discovery of room-temperature luminescence phenomena,[15] has been the subject of much interest, as shown by several conference proceedings.[16] Furthermore, porous silicon is a unique example of a crystalline porous material possessing the structural properties of a nearly perfect single crystal: high-resolution x-ray-diffraction experiments on PS (Refs. 17–19) gave detailed information on strain variations induced by various effects such as oxidation[20] and Ge filling.[21] Recently we also reported x-ray observations of PS strains induced by alkane wetting[22] and vapor adsorption.[23]

In Sec. II of this paper, we give a description of our x-ray measurements of PS strains induced by pentane vapor adsorption. In Sec. III, we review previous explanations of adsorption strain in other materials, and then in Sec. IV we discuss our results for PS in relation to these works. Finally in Sec. V we evaluate the effects of the softening of the elastic constants of PS on adsorption strains.

II. EXPERIMENTAL STUDY OF ADSORPTION STRAINS

A. Properties of porous silicon

Porous silicon is obtained by the electrolysis of a single-crystal silicon wafer in a HF solution producing a thin porous layer on the wafer surface:[24] the porosity and the pore morphology depend on wafer doping, HF concentration, and current density; the porous layer thickness, usually in the μm range, is proportional to the electrical charge. For our work, PS layers with two boron doping levels, both of 10-μm thickness, have been fabricated on (001) silicon wafers under dark conditions. The heavily doped p^+-type samples were fabricated on a wafer of 0.01-Ω cm resistivity, under electrochemical conditions giving a layer of 80% porosity (electrolyte composition: 15% HF, 35% water, and 50% ethanol; the current density is 80 mA/cm^2). The lightly doped p-type samples were prepared on wafers of 5-Ω cm resistivity, with conditions corresponding to 70% porosity (electrolyte composition: 25% HF, 25% water, and 50% ethanol, and a current density of 20 mA/cm^2). It is well known[25,26] that these
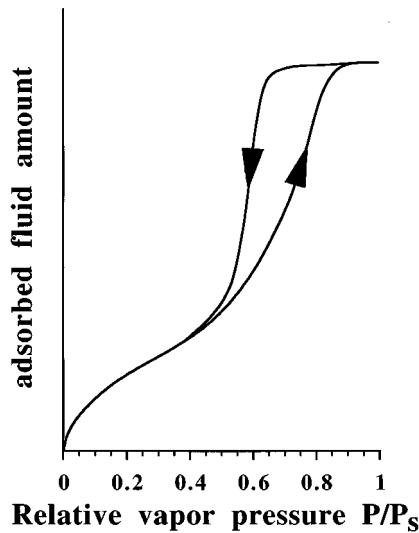
FIG. 1. Schematic representation of the isotherm adsorption (amount of adsorbed fluid vs the vapor pressure relative to the saturation vapor pressure) for a p^+-type porous silicon sample: a hysteresis loop between increasing and decreasing vapor pressure is clearly evidenced at high pressure values.

two types of PS samples exhibit different pore morphologies: p^+-type porous silicon has an anisotropic structure of cylindrical pores, of about 10-nm diameter, with axis parallel to the $\langle 001 \rangle$ direction; p-type PS has a rather isotropic structure of spherical pores of about 3-nm diameter. These results were first obtained by direct electron microscopy observations,[25] while more quantitative results on pore size distributions were deduced from nitrogen adsorption measurements;[26] as these latter measurements are closely related to our work on adsorption strains, we briefly recall some of these results. Vapor adsorption is the classical technique to determine the characteristics of porous materials quantitatively:[2] the amount of vapor, usually N_2 at 77 K, adsorbed in a porous material, is measured versus the vapor pressure. The schematic shape of an adsorption curve, similar to those obtained in p^+-type PS,[26] is shown in Fig. 1: the most striking feature is the presence of a hysteresis loop between increasing and decreasing pressure which, as discussed in Sec. IV C, is related to the capillary condensation of the vapor inside the pores.

B. X-ray-diffraction measurements

1. Experimental setup

X-ray-diffraction experiments were performed with a high-resolution diffractometer (Philips MRD), using a four-reflection Ge monochromator for the Cu $K\alpha_1$ line from an x-ray tube.[20] Typical x-ray rocking curves, obtained for a p^+-type sample by rotations of the sample angle ω, are shown in Fig. 2(a). Around the (004) silicon reflection, two narrow diffraction peaks are detected: one (S) is produced by the silicon substrate, and the other (L) by the porous layer. The lattice mismatch parameter $\Delta a/a$, in the direction perpendicular to the (001) sample surface, is directly proportional to the angular splitting $\Delta\omega$ between the two peaks, according to $\Delta a/a = -\cot\omega_B \Delta\omega$, where ω_B is the Bragg angle for the (004) reflection.[17–20]
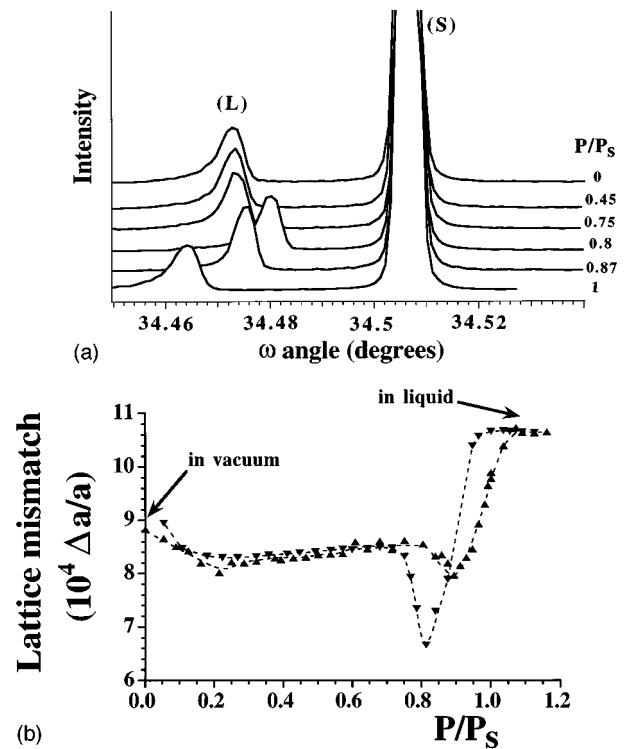
FIG. 2. (a) X-ray rocking curves (intensity vs the angle of rotation ω of the sample) for the (004) reflection of a porous silicon sample (p^+ type, porosity of 80%, 10 μm thick) during pentane vapor adsorption. The vapor pressure P decreases from the saturation vapor pressure P_S to $P=0$. (b) Variation in the lattice parameter mismatch $\Delta a/a$ of the same p^+-type porous silicon sample during pentane adsorption (▲) and desorption (▼) as a function of the relative pressure P/P_S.

X-ray data were obtained at room temperature, with the sample in a vacuum cell with a beryllium window. Pentane vapor was introduced by controlled steps, giving a variable pressure between zero and the saturation vapor pressure of pentane $P_S = 60$ kPa. Caution should be taken to prevent contamination by pump oil, which occurs frequently in vacuum measurements;[27] for our x-ray measurements, contamination by pump oil gives rise to an irreversible decrease of the PS lattice parameter, which was suppressed by using liquid nitrogen traps between the pump and the vacuum cell.

2. Results on p^+-type samples

Rocking curves obtained under various vapor pressures of pentane, for the p^+-type porous silicon sample of 80% porosity, are plotted in Fig. 2(a); the corresponding variation of the lattice mismatch parameter $\Delta a/a$ as a function of the relative pressure P/P_s is plotted in Fig. 2(b). At $P=0$, the lattice expansion of the porous silicon layer $\Delta a/a$ is 8.8×10^{-4}, the same value as in air. This initial expansion is attributed to the effect of the hydrogen coverage of the pore surface, as proposed by Sugiyama and Nittono.[28] With increasing vapor pressure, there is little variation of the rocking curve shapes, up to $P/P_s \approx 0.8$–0.9, where the porous peak broadens and shifts toward the substrate peak, reaching its maximum variation at $P/P_s \approx 0.9$. Around $P \approx P_s$, the porous peak has shifted back, but has not reached the position

TABLE I. Experimental and calculated values of the adsorption strains for different porous silicon samples. The calculations were performed using equations (10) and (11) for p- and p^+-type porous silicon samples, respectively. The ratio between experimental and calculated values is nearly constant.

Sample type and porosity	Liquid and surface tension (mJ/m^2)	Strain at $P = P^*$ ($\Delta a/a \times 10^4$)		
		experimental value	calculated value	calculated/ experimental
p^+ 60%	cyclohexane 25	1.2	2.5	2.1
p^+ 60%	pentane 14	0.7	1.4	2.0
p^+ 70%	pentane 14	1	2.5	2.5
p^+ 80%	heptane 20	2.8	8.0	2.9
p^+ 80%	pentane 14	2	5.6	2.8
p^+ 90%	pentane 14	6.3	22.5	3.6
p 70%	pentane 14	20	68	3.4

found for full immersion in the liquid.[22] The peak width is also slightly larger, showing the presence of a broadening induced by inhomogeneous strains. It is necessary to increase P above P_S (by slightly heating the liquid reservoir above the temperature of the sample) to obtain a full wetting of the PS sample, with a narrow peak and a larger shift, as found during full immersion of the sample in the liquid; this puzzling phenomenon is discussed below in Sec. IV A. With decreasing pressure, i.e., during controlled drying, a strain hysteresis is clearly observed, as shown in Fig. 2(b): the decrease of the lattice parameter occurs at a smaller value, $P/P_S \approx 0.8$, than for increasing pressure. One can note that the $\Delta a/a$ variations occur nearly in the same range as the large variations of adsorption in the hysteresis loop of Fig. 1. As discussed below in Sec. IV C, both effects are attributed to capillary condensation. Other measurements, of the room-temperature-induced strain adsorption of various vapors (mainly of pentane and cyclohexane) performed for various p^+-type PS samples, with porosities between 60% and 90%, show similar hysteresis cycles, with results given in Table I.

3. Results on p-type samples

Larger variations are observed for p-type PS: Fig. 3(a) shows the pressure variation of the rocking curves for increasing pressure, while Fig. 3(b) exhibits the variation of the lattice parameter mismatch versus the pentane vapor pressure. For pressure P increasing from zero, there is first a linear decrease of $\Delta a/a$ with a large broadening of the diffraction peak. Around $P/P_S \approx 0.5$, the porous layer peak is greatly broadened, and is roughly centered around the substrate peak, i.e., $\Delta a/a \approx 0$. Then for increasing pressure, the porous peak shifts back, but remains broad; here, also, it is necessary to have P larger than P_S, to obtain again the narrow peak found during immersion in the liquid.[22] No hysteresis is observed for p-type samples. Although the accuracy
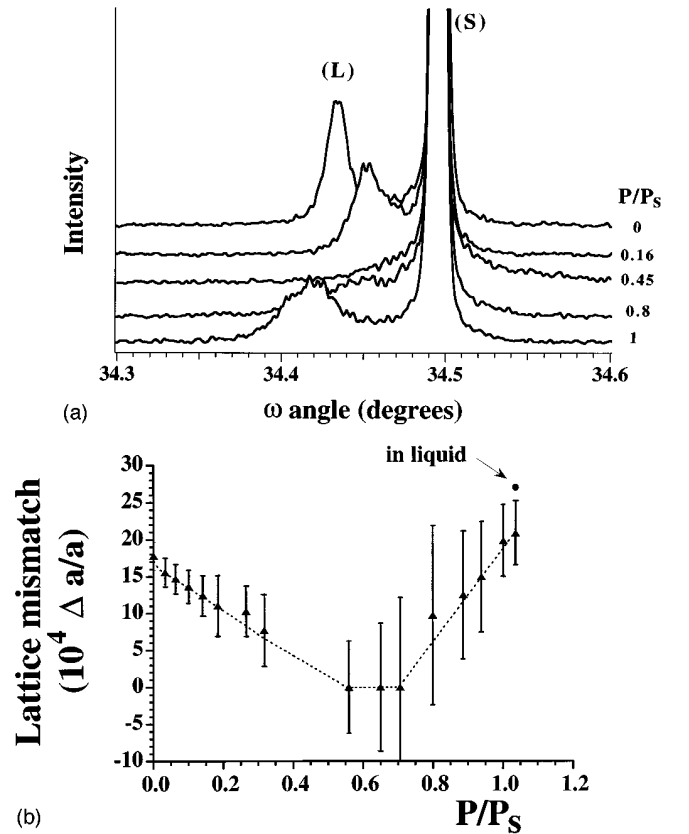
FIG. 3. (a) X-ray rocking curves for the (004) reflection of a porous silicon sample (p type, porosity of 70%, 10 μm thick) during pentane vapor adsorption. The vapor pressure P increases from $P = 0$ to the saturation vapor pressure P_S. (b) Variation in the lattice parameter mismatch $\Delta a/a$ of the same p-type porous silicon sample during pentane adsorption as a function of the relative pressure P/P_S. The dashes at each point represent the full width at half maximum of the x-ray rocking curves. The last point ($\bullet$) was obtained after a slight heating of the liquid reservoir. The dashed line is a guide for the eyes.

of the measurements is reduced by the large broadening of the porous peak, the absence of hysteresis has been observed in several samples. One can also recall that in previous vapor adsorption measurements on p-type samples, similar results were observed: in one measurement, only a very small hysteresis was observed near saturation,[26] while in another measurement no hysteresis was detected.[29]

In conclusion, these results show that adsorption strains are clearly visible in PS, and are quite different for p^+- and p-type PS samples: in p^+-type PS, the strain follows the behavior of the usual adsorption curve of Fig. 1, and shows a well-defined hysteresis; in p-type PS, for increasing pressure, there is a large contraction, followed by an expansion; an important feature is the absence of hysteresis in p-type samples. Finally, both p^+- and p-type samples show an unexpected delay in strain variations around P_S.

III. ADSORPTION STRAINS AND SURFACE THERMODYNAMICS

Before discussing our experimental results on PS strains, we first recall some surface thermodynamics concepts which

have been used to interpret previous measurements of adsorption strains in charcoal and in porous silica. In earlier observations of adsorption strain, only an expansion (or swelling), was observed:[7,8] Bangham and co-workers[6] found that the swelling $\delta\ell/\ell$, measured by dilatometry, was proportional to the two-dimensional surface pressure Π of an adsorbed fluid film. Basic considerations of surface thermodynamics,[30] first developed for fluid interfaces, show that upon adsorption, Π is equal to the decrease of the surface energy $\gamma_{SO} - \gamma_{SV}$ (where the subscripts SO and SV correspond, respectively, to a clean surface under vacuum and to a surface with an adsorbed layer in thermodynamical equilibrium with the vapor at pressure P). Then, assuming that the vapor behaves like a perfect gas, one obtains the classical Gibbs relation

$$\Pi = \gamma_{SO} - \gamma_{SV} = RT \int_0^p \Gamma \, d \ln p \qquad (1)$$

where Γ is the adsorbate excess surface quantity. While the approximation of perfect gas behavior can lead to some quantitative deviations, the prediction of an expansion upon vapor adsorption cannot be escaped, at least if the concepts used for a fluid-fluid interface can be extended to a fluid-solid interface. The explanations of Bangham and co-workers,[6] based on the Gibbs relation, has indeed been used in nearly all the explanations of adsorbent swelling.[7,8] The main problem is then to determine the pore shapes and surface area, and to calculate the effect of the elastic constants of the porous medium. Most often drastic simplifications are used, considering only solid particles with simple geometric shapes (sphere or revolution cylinder) and with isotropic elastic constants. The case of a spherical particle of radius r and of surface energy γ_S is rather simple:[7] according to the Laplace relation, the particle is submitted to a compressive pressure

$$\Delta P = 2\gamma_S / r. \qquad (2)$$

Then there is an isotropic strain ε,

$$\varepsilon = -\Delta P / 3K = -2\gamma_S / 3Kr, \qquad (3)$$

where K is the bulk modulus of a macroscopic sample. The maximum value of γ_S is γ_{SO} for a clean surface under vacuum, producing the larger initial contraction; with vapor adsorption, γ_S decreases, and the particle swells relative to the vacuum state.

Since the review by Sereda and Feldman[8] in 1967, few new works on swelling have been published. We can mention the results of Dash et al.[9(a)] on a material composed of graphite particles with a thick disk shape, and the study of Scherer[31] on a model of porous silica with perpendicular cylindrical pores of uniform radius; these two studies give an expansion proportional to γ/Kr, as in Eq. (3), but with numerical coefficients which depend on pore shapes and on the Poisson ratio of the materials.

Although swelling is the only effect expected from Gibbs Eq. (1), adsorption induced contractions have been observed in many experiments, first in charcoal[32,33] and then in porous silica.[7,34] In fact, as for porous silicon, the observation of adsorption contraction by Haines and McIntosh[32] revealed different behaviors in two pressure ranges:

(a) At high pressure ($P/P_S > 0.4$), there is a contraction with a pressure hysteresis similar to that observed in Fig. 2 for p^+-type PS, which is attributed to capillary condensation of the fluid in the pores, as discussed in Sec. IV C.

(b) At low pressure, there is often a reversible contraction, similar to that of the p-type sample in Fig. 3, called ''anomalous'' by Sereda and Feldman.[8] Various explanations of this anomalous contraction were already proposed by Haines and McIntosh in their first paper on contraction:[32] anisotropic strain, dissolution of the adsorbate in the adsorbent, and capillary condensation in narrow crevices. Subsequently two other explanations were proposed: for charcoal, bridging of adsorbate molecules between two closely spaced walls;[35] and for porous silica, H bonding at specific sites, probably SiOH groups, on silica surface.[7] More recently, two general explanations of adsorption contraction have been proposed: one by Ericksson,[13] based on the rigorous thermodynamics of a plane solid surface, and the other by Ash, Everett, and Radke,[14] for a fluid confined between two parallel planes.

(i) In 1969, Ericksson published a thermodynamic analysis of adsorption strain taking into account the specific properties of a solid surface.[13] For a solid surface, the concept of surface tension used for a fluid is ambiguous, and one has to distinguish between the surface free energy γ and the surface stress tensor σ_{ij}. According to the Shuttelworth relation,[36] the relation between γ and σ_{ij} is given by

$$\sigma_{ij} = \gamma \delta_{ij} + d\gamma / d\varepsilon_{ij}, \qquad (4)$$

where δ_{ij} is the Kronecker symbol and ε_{ij} is the surface strain. For a fluid surface there is no variation of the surface energy as a function of strain, and σ is numerically equal to γ. Ericksson showed that, for a solid surface, different behaviors are expected for mobile adsorbed molecules (as in a fluid film) and for localized adsorption (as in a solid film). For a fluid film on a plane solid surface, the change of surface stress is equal to the decrease of the surface free energy, given by Gibbs Eq. (1); then, for a smooth solid surface, the adsorption of a fluid layer can only produce a swelling of the adsorbent. On the other hand, localized adsorption of molecules with lateral interactions can lead either to a contraction or to an expansion, according to the values of the interaction parameters. In this case of localized adsorption, which occurs mainly at low temperature, a statistical mechanical model shows that, with increasing pressure, a temperature-dependent crossover from contraction to expansion can occur for coverages less than a complete monolayer. This treatment was extended by Hasley,[37] to the case of a transition from a commensurate to an incommensurate crystalline layer, or to the case of melting of a crystalline layer. Indeed, with increasing pressure, Beaume et al.[9(b)] observed a discontinuous expansion at the liquid-solid transition of a CH_4 layer adsorbed on a graphite adsorbent. They explained the observation of an initial contraction by the heterogeneous adsorption of the first fractions of a layer in strongly interacting sites, while the expansion at higher pressure is explained by the usual decrease of the surface energy, produced by the adsorption of a fluid layer.

(ii) Another approach of adsorption strain was proposed in 1974 by Ash, Everett, and Radke,[14] who considered the thermodynamic behavior of a fluid confined between two

parallel plane walls. In addition to the usual thermodynamic parameters (entropy S, volume V, and number of atoms N), they introduced two supplementary parameters; the wall area A and the wall distance h. With these parameters, the variation of the system energy can be written as

$$dU = TdS - PdV + \mu dN + 2\sigma dA - Afdh. \qquad (5)$$

This formulation, which includes the effects of the surface stress σ conjugate to the surface area A already considered by Ericksson,[13] introduces an effect with the existence of a force f conjugate to the distance h between the two walls. In vacuum, the force f is the van der Walls attraction between the two walls.[4] In the presence of a low-pressure gas, there are thin adsorbed layers on the two walls; the dispersion forces between these two layers increase the attraction between the walls. With a liquid between the walls, a more complex behavior is observed: at a large distance there is again an attraction; but for short distance (of a few molecular diameters) an oscillating interaction is observed in experiments[4] as well as in computer simulations.[38] Balbuena, Berry, and Gubbins[39] made a detailed simulation of the force variations between two parallel walls as a function of the pressure and distance between the walls. For a distance of a few molecular diameters, there is first an attraction increasing with the pressure; then there is a capillary condensation, marked by a discontinuous increase of the attraction; finally, at higher pressure in the liquid phase, there is generally a repulsion between the walls. These considerations are directly related to recent measurements of capillary condensation with a surface force apparatus.[40]

The extension of these ideas to adsorption in the more complex geometry of real porous materials is not easy. Ash, Everett, and Radke[14] made a qualitative discussion of adsorption strain, with a competition between the expansion due to the decrease of surface energy and the contraction due to the contribution of dispersion forces in the presence of adsorption. Recently, progress has been made in theoretical studies of adsorption in pores of simple shapes, using either a macroscopic approach for circular cylinders[41] and concave wedges,[42] or a microscopic description, also in cylinders[43] and in wedges.[44] However, to the authors' knowledge, no analysis of adsorption stress has been published so far in these two situations.

This brief presentation shows that the application of surface thermodynamics to solid surfaces is far more complex than for liquids. Several mechanisms can lead to a contraction of a porous adsorbent. However, for adsorbed fluid layers, it seems that a low-pressure contraction can only be explained by attractive dispersion forces acting on molecules adsorbed on walls separated by very short distances. For higher pressure, the normal swelling due to the decrease of surface energy generally occurs.

IV. STRAINS DUE TO THE INTERACTION OF POROUS SILICON WITH A FLUID

In this section we will apply previous considerations of surface stress for a discussion of our experimental results on the variations of PS strains under the influence of various fluids. First, in Sec. IV A, we discuss the usual swelling phenomena expected from the decrease of the surface energy;

then we consider the origin of the contraction phenomena observed at low and high pressure, in parts Secs. IV B and IV C, respectively.

A. Swelling of porous silicon

1. Initial expansion of as-formed samples

Before considering adsorption swelling, we first discuss the origin of the initial expansion of as-formed samples. Since the work by Barla et al.,[17] it has been known that the lattice parameter of p^+-type PS is larger, by a few 10^{-4}, than that of the bulk silicon substrate. For p-type PS, Young, Beale, and Benjamin[45] found a larger expansion of a few 10^{-3}. Recently we have discussed the various models proposed to explain the initial expansion of PS,[19] and we think that the explanation of Sugiyama and Nittono,[28] who attributed this effect to the presence of hydrogen on the PS surface, is the most probable. We note that the expansion observed in PS is a rather peculiar phenomenon, as usually small crystalline particles show a contraction.[46] However the H coverage results from chemical interactions during PS fabrication, producing stable SiH bonds, very different from the physical adsorption of alkanes on silicon considered in this paper. Then, following Ericksson,[13] for localized chemisorption an expansion of the substrate can be observed for suitable values of atomic interactions. This initial expansion of PS is also in agreement with the calculation of Itoh et al.[47] of the average Si-Si distance in silicon clusters with a surface coverage of hydrogen (however, these clusters are too small to present a crystalline structure). Another effect which can increase the initial expansion is the presence of an oxide layer, a phenomenon which we have studied in detail in the case of anodic oxidation.[48]

Heating of a PS sample in vacuum above 350 °C produces hydrogen desorption. This thermal annealing produces a contraction of the lattice parameter by a few 10^{-3}, which may correspond to the usual contraction, due to the effect of the surface energy on a clean crystallite, given by Eq. (3). With $K = 98$ GPa (Ref. 49) and $\gamma_S = 1.25$ J/m^2 determined from a cleaving measurement under vacuum,[50] one obtains a contraction of 2.6×10^{-3} for $r = 3.3$ nm. However, the contractions following H desorption were measured in air at room temperature, on samples probably already covered by a water or a pollution layer. Further measurements under ultrahigh vacuum would be very interesting to determine the real value of this contraction.

2. PS swelling in the presence of a fluid

The melting temperature of pentane is 143 K,[51] and as usual this melting temperature decreases in a confined volume,[52,53] pentane adsorption under ambient conditions leads to a fluid film. Then, following Ericksson,[13] for a solid particle with a smooth surface covered by a fluid film, one can only expect an expansion of the adsorbent. The decrease of the surface energy produced by vapor adsorption, up to saturation pressure, is given by the Gibbs Eq. (1). A further decrease of the surface energy is produced by a full immersion in a fluid, as indeed observed by Bangham and Razouk in charcoal,[54] in one of the rare measurements of this effect.

However, the results obtained for porous silicon are rather different from the expected continuous swelling: in p-type

samples the main effect is a large contraction at low pressure, which will be discussed in Sec. IV B; in the p^+-type sample there is mainly a plateau until the contraction due to capillary condensation around $P/P_S=0.9$, discussed in Sec. IV C. In both kinds of samples, there is a final expansion for a complete wetting. We now consider the value of the swelling of PS expected from the decrease of surface energy due to adsorption and wetting.

For this we have to consider the variation of the surface energy of a solid in the presence of a liquid and of its vapor, a problem first studied by Bangham and Razouk[55] for the adsorption swelling of charcoal. They also extended this approach to a determination of the contact angle of a liquid on a solid following the Young equation[30]

$$\gamma_{sv} - \gamma_{sl} = \gamma_{lv}\cos\theta, \qquad (6)$$

where θ is the contact angle and the subscripts s, l, and v refer to solid, liquid and vapour respectively. Bangham and Razouk[55] pointed out that at thermodynamic equilibrium, the solid surface outside the liquid drop is covered by a film due to vapor adsorption; the surface energy in Eq. (6) is γ_{sv} and not the vacuum surface energy γ_{so} used above. The surface energy variation $\gamma_{so} - \gamma_{sv}$ is given by the Gibbs equation (1). The total variation of the surface energy for immersion of a clean surface is obtained by adding the contribution of Eqs. (1) and (6), giving

$$\gamma_{so} - \gamma_{sl} = RT\int_0^p \Gamma d \ln p + \gamma_{lv}\cos\theta. \qquad (7)$$

The maximum value is obtained for full wetting with $\cos\theta=1$, the only case which we consider below. Typical values of these two contributions for crystalline SiO_2 powders were determined by Boyd and Livingston:[56] for water they found the contribution due to vapor adsorption to be about 250 mJ/m^2, with a final wetting contribution $\gamma_{lv}=73$ mJ/m^2. For heptane, the corresponding contributions were 40 and 20 mJ/m^2, respectively. The interaction between a solid and an alkane is only due to van der Walls interactions,[4] while between water and silica there are also short-range hydrogen bonds between H_2O and the OH groups present at the silica surface.[57] In the modern theory of wetting, these interactions are called Lifshitz–van der Waals and acid-base interactions,[58] respectively.

We now study how these considerations can be applied to adsorption and wetting of bulk silicon, two phenomena which depend greatly on the surface chemistry and roughness of the samples. Traditionally, in silicon technology, oxidized silicon wafers are considered hydrophilic, while HF etched wafers are considered hydrophobic.[59] However, as sketched below, recent works show more complex properties.

Oxidized silicon. A clean silicon surface obtained by cleavage or after ultrahigh-vacuum thermal annealing is unstable at room atmosphere, and is quickly covered by a native oxide layer of about 2 nm thick, while thicker oxides of better quality are produced by various oxidation processes (thermal, anodic, chemical, etc.).[60] Although these oxidized surfaces are often considered hydrophilic, i.e., with a water contact angle $\theta=0$, finite contact angles between 40° and 70° are often found,[61] with large variations depending on the

sample history. Such contact angles can conveniently be used to characterize silicon surface cleanness. In agreement with the results of William and Goldman,[59] the interaction of fluids with silicon wafers covered by an oxide layer thicker than a few nm is identical to that of bulk silica.[57] In both cases, the presence of OH groups on the oxide surface has a great effect on the wetting properties.

The surface properties of oxidized silicon are also very important for vapor adsorption measurements, as shown by the recent ellipsometric measurements of Beaglehole and Christenson[62] on flat silicon surfaces: for water the adsorption is small, with only a thin liquid layer at P_S; for pentane, there is first a linear adsorption regime for P/P_S smaller than 0.5; closer to P_S, there is a large increase of the adsorption layer thickness, pointing to a nearly continuous wetting behavior. For cyclohexane, Lawnick et al.[63] even reported the existence of a wetting transition, i.e., the observation of a change from a thin to a thick liquid layer around 20 °C. They also interpreted the linear variation of low-pressure adsorption as an evidence for a weak adsorption by small size inhomogeneous structures. However, the change of surface energy in these recent experiments were not presented.

H-covered silicon. After HF etching, silicon is covered by SiH_x, with properties depending greatly on the pH of the etching solution and on surface orientation.[64] For the perfect Si(111) surface, water contact angles from 40° to 90° have been measured, depending on surface preparation conditions.[65] This is mainly due to the modification of the H bonding possibilities existing with the OH groups of silica which are suppressed when the silicon atoms are passivated by hydrogen. On the other hand, van der Walls interactions of alkanes with silicon and silica have, within a factor of 2, the same amplitude, although the exact value is unknown due to the large incertitude for the value on the silica Hamaker constant.[66]

In conclusion, silicon surfaces, either oxidized or hydrogenated, often present a finite contact angle with water, which corresponds to the behavior of a low-energy surface. In the case of an oxidized surface, this is due to a small concentration of OH group after high-temperature treatments. SiH-covered surface behaves probably also as a low-energy surface with little adsorption.

Wetting of PS. The surface of fresh as-formed PS is mainly covered by SiH_x and is usually considered hydrophobic,[67] while an oxidized sample will present more hydrophilic properties. Considering only a fresh sample, the linear variation of strain versus vapour pressure in a p-type sample recalls the linear adsorption regime of alkanes on oxidized bulk silicon.[62,63] As both effects are due only to van der Walls interactions, we can use the conclusion of Lawnik et al.:[63] that is, due to a small adsorption by a surface nonhomogeneous at nanometric distances. In this picture of a low-energy surface the main effect of vapor adsorption occurs with the growth of a macroscopic liquid film above P_S, producing a decrease of the surface energy on the order of γ_{lv}. For pentane, with a surface energy $\gamma_{lv}=15$ mJ/m^2, this wetting leads to a swelling from 10^{-5} to 10^{-4} for a silicon particle of radius from $r=10-1$ nm, a result which is smaller than the experimental value by about an order of magnitude.

3. Behavior around saturation vapor pressure

Finally we discuss the unexpected behavior observed around the saturation vapor pressure P_S. In principle, with long-range van der Walls interactions, one would expect a continuous wetting at P_S. However, for the two kinds of samples studied (p and p^+ types), broad diffraction peaks are observed at P_S with a lattice parameter smaller than for complete wetting (even after waiting a dozen hours); it is necessary to go to higher vapor pressure to obtain an external liquid film, which is able to equalize the internal pore pressure giving a narrow peak such as that found for immersion. Similar wetting anomalies have been observed in the past, for vapor-saturated charcoal: Bangham and Razouk[54] observed that a charcoal sample filled with methyl alcohol at P_S exhibits a supplementary expansion when immersed in the liquid. Several explanations of these effects are possible:

(i) One possibility is that for $P = P_S$, the fluid pressures are not equal in different pores or at least in various subsystems of pores: this supposes that nonequilibrium spherical menisci are present, and that there is no internal pressure equilibrium between different pores: the presence of menisci with different curvature can be due to a hysteresis of the contact angle, an effect well known for forward and backward motion of a liquid drop[68] on an inhomogeneous surface. The presence or absence of a transversal pore connectivity in as-formed electrochemically produced PS samples is not well documented; we know of no direct investigation of pore connectivity; we found only a brief mention of the absence of internal pore connections in a review paper.[69] However, for samples thinned by chemical dissolution, which occurs with a constant dissolution rate, thin pore walls will be easily perforated.

(ii) Another possibility could be that the external surface has wetting properties different from those of the internal pore surface, or that the growth of a macroscopic thick film is a discontinuous process occurring only at a finite pressure above P_S. But recent experiments[62] have shown that pentane adsorption on a flat Si substrate produces a thick (25 nm) film at P_S. However, there are major differences in the chemistry and morphology of external silicon surfaces, between PS and a bulk silicon wafer: a polished Si substrate has a very smooth surface and is covered by a thin native oxide film, of about 2 nm thick; on the other hand, the PS surface is pierced by many pore orifices, and may be rough at the atomic scale; furthermore the PS surface is covered by SiH_x and not by SiO_2. On such a rough surface, the first capillary condensations probably occur below P_S in the depressions of the external surface[70] or around pore orifices. On the other hand, the wetting of surface ridges will be more difficult, and will occur only at a finite pressure above P_S. Similar delays are expected from the work of Schrader and Weiss[71] on the nucleation of a liquid drop on a flat solid surface.

(iii) Another possibility is that an equilibrium state was not reached at P_S. Indeed a long time of one week has been reported for the complete adsorption of pentane vapor by charcoal at P_S.[72] Recently, time-dependent studies of wetting on smooth surfaces have been performed with x-ray reflectometry:[73] after a small temperature perturbation the return to equilibrium follows an exponential variation with time constants larger than one day. It is then possible that our waiting time of 12 h was not long enough to reach equilibrium, although, for pressure smaller than P_S, sample strains were stable after a few minutes.

Further studies are needed to clarify the behavior of PS adsorption strain around P_S; but we note that these phenomena, which are easily observed in macroscopic or X-ray diffraction strain measurements, would be rather difficult to detect in usual adsorption measurements, where only the small volume variations related to the filling of meniscus concavity at the pore end will be measured.

B. Low-pressure contraction of porous silicon

For low vapor pressure, reversible contractions are observed in PS: a small contraction for p^+-type samples, a larger one for p-type samples. As proposed by Ash, Everett, and Radke,[14] this contraction can be due to the van der Walls attraction between two opposite walls which increases when they are covered by a thin liquid film. Grüning and Yelon[74] also considered the effect of van der Waals attractions in relation to their measurements of PS strain during drying. As described in the book by Israelachvili,[4] the van der Waals attraction depends on the shape and size of the interacting objects. To give the order of magnitude of such effects, we can consider the interaction energy E between two thick parallel plates, separated by a distance d, which is given by $E = A/12\pi d^2$, where $A = 2.7 \times 10^{-19}$ J is the Hamaker constant of silicium;[64] then, for $d = 1$ nm, $E = 7.2$ mJ/m^2.

However to produce a contraction, this attraction must be larger than the usual expansion due to the reduction of the surface energy given by Eq. (1). In Sec. III A, we showed that for liquids with only a van der Waals interaction, this effect is often of the order of the surface tension of the liquid, which for pentane is around 15 mJ/m^2. Then in order to observe a contraction at low vapor pressure, the van der Waals attraction energy should be of a similar value, which can occur only with structure size in the nm range.

The observation of such small size features is a difficult question which has not been completely clarified for p-type PS, as such structures are below the detection limits of classical measurement techniques: for nitrogen adsorption measurements,[27] the resolution is limited to $r = 1.5$ nm, by the tensile strength limit of liquid nitrogen.[2,75] Several electron microscopy observations of PS have been published, showing features of a few nm size;[25,76] but smaller three dimensional objects are very difficult to detect by electron microscopy. Recently, extended x-ray-absorption fine-structure measurements were explained by the existence of very small particles of crystalline silicon with sizes as small as 1.3 nm.[77] Then, supposing that pores and silicon crystallites have similar sizes in the nm range, one can expect that the contraction observed in p-type PS may be related to the effects of attractive van der Waals interactions.

The role of crevices or of small cavities, which are preferential structures for vapor adsorption, has often been mentioned to explain the existence of a contraction qualitatively. For the larger size, as developed below in Sec. IV C, a confined liquid is separated from the vapor phase by a concave meniscus, which according to the Laplace relation [Eq. (2)] produces a negative pressure in the liquid which leads to a contraction of the adsorbent. For smaller sizes, of the order of a few molecular diameters, a sharp meniscus does not

exist,[2] but the contraction effect due to the attractive dispersion forces between the adsorbed molecules and the walls of a small cavity is probably always present.

C. Capillary condensation at high pressure

1. Capillary condensation in porous materials

The existence of an adsorption hysteresis is an old problem,[78–80] always under active investigation.[3] It has been known for a long time that adsorption hysteresis is associated with capillary condensation inside the pores: under thermodynamic conditions, where the vapor is stable in a large volume, the liquid phase can condense in a confined volume, and is then separated from the vapor phase by a meniscus. As shown in Fig. 1, there is a hysteresis between the filling and emptying of a porous structure. The origin of this capillary condensation hysteresis can be attributed to two kinds of phenomena:

(i) Percolation of the vapor phase (during evaporation) inside a statistical network of pores,[81] where a continuous gas-liquid interface penetrates inside the pores.

(ii) The instability of an adsorbed layer in a single cylindrical pore with open ends;[82,83] under increasing vapor pressure, the thin liquid layer adsorbed inside a cylindrical pore becomes unstable, leading to pore filling, with nucleation of a spherical meniscus. In the following, we will consider only the instability in a single pore.

When the liquid and vapour phases, inside a cylindrical pore, are separated by a concave spherical meniscus of radius r_s, there is a negative pressure in the liquid given by Laplace equation, leading to a contraction of the adsorbent.[8,12] The equilibrium radius r_s of a spherical liquid meniscus, in contact with a vapor at pressure P and temperature T, is given by the Kelvin relation[30]

$$\ln\left(\frac{P}{P_s}\right) = \frac{-2v\,\gamma_{LV}}{r_s RT}, \tag{8}$$

where v is the molar volume of the liquid. When there is a complete wetting of the porous material by the liquid, i.e., when the contact angle θ is zero, the stability limit of the meniscus, under decreasing pressure, occurs at a pressure P°, where the meniscus radius r_s is equal to the pore radius r_p; the pore radius r_p can then be determined from the shape of the adsorption curve using the Kelvin equation. On the other hand, for increasing pressure, there is a delay for the nucleation of a spherical meniscus inside a cylindrical pore with open ends, which leads to a pressure hysteresis, as proposed by Foster.[78(a)] In a more quantitative way, Cohan[79(a)] considered that for increasing pressure, the vapor is in equilibrium with a cylindrical meniscus of curvature $1/r_c$ (which is different from the curvature $2/r_s$ of a sphere). This leads to a modified Kelvin equation

$$\ln\left(\frac{P}{P_s}\right) = \frac{-v\,\gamma_{LV}}{r_c RT} \tag{9}$$

First, Cohan considered that the meniscus nucleates at a pressure P^*, where $r_c = r_p$; with this simple hypothesis, the instability values of $\ln(P/P_s)$, for increasing and decreasing pressure, are related by a factor 2. However to take into account the presence of an adsorbed layer of thickness t on the pore walls, Cohan[79(b)] proposed that $r_c = r_p - t$. Later, it was understood that such a liquid film layer can be stabilized only under the effect of an attractive potential from the pore walls,[78(b),83] and that the layer thickness is also dependent on the vapor pressure. Recently computer simulations of meniscus nucleation in narrow pores were performed for molecules interacting with Lennard-Jones potential:[84] it was found that the capillary condensation hysteresis due to meniscus nucleation depends greatly on the pore geometry (slit or cylinders) and on the shape of pore ends, either open or closed.

2. Application to porous silicon

$p+$ type. Due to a larger pore size and maybe to a more homogeneous structure, the hysteresis cycle is more distinctly observed in p^+-type materials, for adsorption measurements[26] as well as for the x-ray strain measurements reported in this paper. For the p^+-type PS sample, the decrease of the lattice mismatch $\Delta a/a$ observed in Fig. 2(b) corresponds to the steep rising parts of the schematic adsorption loop of Fig. 1, in a range where the menisci are moving inside the pores. The minimum of $\Delta a/a$ for desorption is around $P^\circ/P_s = 0.81$, which, according to the Kelvin equation (8), corresponds to a pore radius of 6.0 nm (assuming $\theta = 0$ and neglecting the thickness of the adsorbed layer). This value is in fair agreement with those obtained using direct adsorption measurements,[26] small angle,[85] and diffuse[18] x-ray scattering measurements. For adsorption, the modified Kelvin equation (9) gives $P^*/P_s = 0.90$, in good agreement with the experimental value of 0.89. This result seems to agree with Cohan's model, but as the basis of this model is rather dubious, the agreement is probably fortuitous.

p type. For p-type samples, the pore radius estimation is more uncertain; one can roughly estimate $P^\circ/P_s = 0.5$, which corresponds to a pore radius of 1.8 nm, also in agreement with nitrogen adsorption results.[26] However this is close to the limit of adsorption measurements due to the finite tensile strength of adsorbed liquids.[2,26,48] Another remarkable property of adsorption in very small size structure is its reversibility. It is a well-known experimental fact[2] that adsorption curves, as shown in Fig. 1, are reversible at low pressure, and that the capillary hysteresis loop is observed only for $P/P_s > 0.4$. Furthermore completely reversible adsorption curves are observed in materials with pores in the nm range: for example, reversible adsorption strain similar to those of p-type PS have been observed for pressures between zero and P_s in microporous carbons.[86] Indeed, in a tightly confined pore, the interfacial meniscus between liquid and gas states cannot exist.[3,87] An explanation for this absence of hysteresis is that the liquid cannot support the high tensile stress which would be produced by a meniscus of small radius.[75] Another possible explanation for the absence of a meniscus in small size pores is that the distance between two walls is a thermodynamic parameter which modifies the phase diagram, giving a confinement induced critical point;[87] then, for small pore size, there is a continuous transition between gas and liquid states, and there is no hysteresis related to the nucleation of a meniscus. An even simpler explanation for the absence of hysteresis is that the pores have dead ends with conical shapes, so that the meniscus is easily nucleated without hysteresis in the cone apex.[80]

To conclude, complex effects can be expected from the van der Waals interactions of adsorbed molecules with a solid surface, presenting a complex shape in the molecular size range. Then there is competition between the contraction produced by molecules confined in a small volume and the usual swelling due to the decrease of surface energy. For p-type materials at low pressure, the contraction effect is rather large. For p^+-type materials with larger pores of a few nm diameter, only a small contraction can be observed at low pressure. On the other hand, at higher pressure, the contraction produced by capillary condensation is clearly observed in p^+-type PS, with a distinct hysteresis between increasing and decreasing pressure. The absence of adsorption hysteresis for p-type PS can also probably be related to a pore size in the nm range.

V. EFFECT OF ELASTIC CONSTANT SOFTENING ON ADSORPTION STRAIN IN POROUS SILICON

The amplitude of the adsorption strains results from a competition between the phenomena at the origin of the stress (reduction of surface stress, attraction due to dispersion forces, capillary stresses, etc.) and the opposing elastic stiffness of the porous material, which would be different at different spatial scales.

(i) On the crystallite scale, the swelling is produced by a variation of the surface energy as given by Eq. (3), with the bulk value of the elastic constants.

(ii) On the macroscopic scale, the response of a porous material submitted to a macroscopic deformation is related to the average macroscopic elastic constants of the porous media, which is generally smaller than the bulk value.[88]

(iii) On the pore scale, attractive dispersion forces exist between pore walls, and the corresponding deformation is mainly due to shear strains, occurring mainly in the less rigid parts of the porous structure; the adsorption strains depend not only on the elastic constants of the material but also on pore shape and size (i.e., the local architecture of the material), which would need a complex evaluation.

In this section we make some estimation of adsorption strains of porous silicon in a macroscopic porous sample. It is well known that porous materials have smaller macroscopic elastic constants than bulk materials.[88] This is also the case for PS, as found in previous determinations of elastic constants using x-ray diffraction[17] or acoustic techniques.[89] A recent systematic investigation[90] of PS Young's modulus E_p has been performed by means of the nanoindentation technique, mainly for p^+-type PS samples in a porosity range between 36% and 90%. The results obtained using these three different techniques are in reasonable agreement (when the comparison is possible). The nanoindentation results show that E_p (for p^+-type PS samples) is close to $E_{Si}(1-P)^2$, where $E_{Si} = 166$ GPa (Ref. 49) is the bulk silicon Young's modulus value, and P is the porosity. This quadratic dependence is in agreement with the model of Gibson and Ashby, developed for cellular materials.[88] Moreover it was shown that the E_p value for a p-type sample was lower (by a factor of 5 for the same porosity of 70%) (Ref. 90) than those of p^+ type. The origin of this difference is probably related to the smaller pore and crystallite sizes in p-type samples.

The macroscopic elastic constants must be used for capillary strains during drying, as shown by Scherer in the case of gel drying.[12] The maximum capillary stress ΔP occurs when the menisci enter the pores, and is given in first approximation by the Laplace equation. Then one can assume that Eq. (3) is valid with K replaced by the macroscopic modulus of porous silicon K_p, which is related to the Young's modulus E_p by $K_p = E_p/3(1-2\nu)$ [ν is the Poisson coefficient for which only one estimation was given for PS (Ref. 17): $\nu \approx 0.1$]. Therefore the strain ε is roughly given by

$$\varepsilon \approx \frac{-\Delta P}{3K_p} \approx \frac{-2\gamma_{LV}(1-2\nu)}{rE_p} . \qquad (10)$$

From Eq. (10), it appears clear why adsorption strains are larger for p-type samples than for p^+ type: the average pore size r is smaller (about 1.5 and 6 nm for p and p^+ types, respectively) and the E_p value is lower than those of p^+ type.

Concerning p^+-type layers for which the Young's modulus follows the Gibson and Ashby relation[90] $E_p = E_{Si}(1-P)^2$, then one obtains

$$\varepsilon \approx \frac{-2\gamma_{LV}(1-2\nu)}{rE_{Si}(1-P)^2}. \qquad (11)$$

For pentane ($\gamma_{LV} \approx 14$ mJ/m^2) and for a p^+-type sample of 80% porosity [i.e., when $r \approx 6$ nm and $(1-P)=0.2$], one obtains $\delta(\Delta a/a) \approx 5.6 \times 10^{-4}$. This calculated value has a good order of magnitude, but is higher than the experimental one: at $P/P_S = 0.9$ on Fig. 2(b), where $\delta(\Delta a/a) \approx 2 \times 10^{-4}$. A more accurate calculation would require a more precise structural information.

Similar experiments have been performed either with pentane or other liquids (like cyclohexane for which $\gamma_{LV} = 25$ mJ/m^2) and for a series of p^+-type samples of porosity $P = 60\%$, 70%, 80%, and 90%. The experimental results, given in Table I, reveal that the observed capillary strains have a dependence versus γ_{LV} and P which is in reasonable agreement with Eqs. (10) and (11). The experimental values are lower than the calculated ones, but the ratio between them is nearly the same (between 2.0 and 3.6), even if the strains amplitude cover a range of nearly two orders of magnitude. Moreover it appears that the less stiff PS layers (i.e., p^+ type with 90% of porosity and the p type one) have the strongest ratio value, indicating that this ratio depends on the porous structure.

For the adsorption strain of p-type samples, one can attempt a calculation using Eq. (10) with $r \approx 1.5$ nm and $E_p = 2.2$ GPa for 70% porosity.[90] Although the existence of a meniscus is dubious for this small size, one obtains $\varepsilon \approx 68 \times 10^{-4}$, also higher than the observed value which is roughly 20×10^{-4} [see Fig. 3(b)]. One observes, moreover, that the x-ray rocking curves broaden for p-type samples due to the inhomogeneous capillary stresses, as shown by Fig. 3(b), where the full width at half maximum is represented.

It is worth noting that these inhomogeneous stresses induced by capillary effects during drying can be quite large, and can even produce a cracking of the porous layer when the porosity or thickness are too large.[91] We have recently studied the mechanisms involved in the cracking of PS

layers.[92] The best way to suppress capillary cracking is to use hypercritical drying, with a pressure larger than the critical pressure of the pore fluid[91] or (in a more easy but less efficient way) by using a drying liquid with a lower surface tension.[92] Freeze drying has also been recently used for porous silicon, leading to encouraging results.[93] Because of the peculiar properties of PS (its nearly perfect crystallinity, for instance) the study of the PS drying can be viewed as a model to obtain a better understanding of the drying of porous materials.

VI. CONCLUSION

In this work we reported the observation of pentane adsorption strains in porous silicon layers. Due to the single-crystal properties of porous silicon, high-resolution x-ray-diffraction measurements allow a direct measurement of the average lattice parameter of the porous layer. Two different behaviors are observed: in a p-type sample with a small isotropic pore structure, there is a reversible low-pressure contraction followed by an expansion. In p^+ samples with a larger cylindrical pore structure, the low-pressure contraction is quite a bit smaller, but is followed at higher pressure by contraction with a hysteresis associated with capillary condensation and with meniscus nucleation. In both cases, there is a final expansion for complete wetting. Further information on inhomogeneous internal strains can be obtained from the broadening of the diffraction peaks. The two kinds of adsorption strains observed in porous silicon are similar to those observed previously in very different porous materials (charcoal and porous silica).

(i) The systematic observations of a contraction followed by an expansion could have a common origin which can only be found in the competition between the expansion due to a decrease of surface energy and the contraction due to dispersion forces attractions in very small cavities, following the proposition of Ash, Everett, and Radke.[14] There is a final expansion for complete wetting.

(ii) Capillary condensation induces a contraction in the large pores, with a hysteresis between increasing and decreasing pressure, which can produce a cracking of the porous layer in the weaker structures. The softening of the elastic constants characteristic of porous materials enhance the magnitude of these deformations.

Studies of these effects in various porous materials enable us to test the validity of the proposed explanations, and to provide additional information on the somewhat neglected subject of adsorption strains. Due to its good crystalline properties, the variety and the easy control of its porous structure, porous silicon can be very useful for such studies.

[1] *Liquids at Interfaces*, edited by J. Charvolin, J. F. Joanny, and J. Zinn-Justin, Les Houches Summer School, session 48 (North Holland, Amsterdam, 1990).

[2] S. J. Gregg and K. S. V. Singh, *Adsorption, Surface Area and Porosity* (Academic, New York, 1982).

[3] R. J. Evans, J. Phys. Condens. Matter **2**, 8989 (1990).

[4] J. Israelachvili, *Intermolecular and Surface Forces* (Academic, New York, 1991).

[5] F. T. Meehan, Proc. R. Soc. London Ser. A **115**, 199 (1927).

[6] D. H. Bangham, N. Fakhoury, and A. F. Mohamed, Proc. R. Soc. London Ser. A **138**, 162 (1932); D. H. Bangham, Trans. Faraday Soc. **33**, 805 (1937).

[7] D. J. C. Yates, Adv. Catal. **12**, 265 (1960).

[8] P. J. Sereda and R. F. Feldman, in *Solid Gas Interfaces*, edited by E. A. Flood (Marcel Dekker, New York, 1967), Vol. 2, p. 729.

[9] (a) J. G. Dash, J. Suzanne, H. Shechter, and R. E. Peierls, Surf. Sci. **60**, 411 (1976); (b) R. Beaume, J. Suzanne, and J. G. Dash, *ibid.* **92**, 453 (1980).

[10] P. Thibault, J. J. Préjean, and L. Puech, Phys. Rev. B **52**, 17 491 (1995).

[11] G. G. Litvan, Adv. Colloid Interf. Sci. **9**, 253 (1978).

[12] C. J. Brinker and G. W. Scherer, *Sol-Gel Science* (Academic, New York, 1990).

[13] J. C. Ericksson, Surf. Sci. **14**, 221 (1969).

[14] S. G. Ash, D. H. Everett, and C. Radke, J. Chem. Soc. Faraday Trans. II **69**, 1256 (1973).

[15] L. T. Canham, Appl. Phys. Lett. **57**, 1046 (1990); A. Halimaoui, C. Oules, G. Bomchil, A. Bsiesy, F. Gaspard, R. Herino, M. Ligeon, and F. Muller, *ibid.* **59**, 304 (1991).

[16] *Microcrystalline and Nanocrystalline Semiconductors*, edited by R. W. Collins, C. C. Tsai, M. Hirose, F. Koch, and L. Brus, MRS Symposia Proceedings No. 358 (Materials Research Society, Pittsburgh, 1995), *Light Emission from Silicon*, edited by J. C. Vial, L. T. Canham, and W. Lang [J. Lumin. **57** (1993)]; *Porous Silicon and Related Materials*, edited by R. Hérino and W. Lang [Thin Solid Films **255** (1995)].

[17] K. Barla, G. Bomchil, R. Hérino, J. C. Pfister, and J. Baruchel, J. Cryst. Growth **68**, 721 (1984); K. Barla, R. Hérino, G. Bomchil, J. C. Pfister, and A. Freund, *ibid.* **68**, 727 (1984).

[18] D. Bellet, G. Dolino, M. Ligeon, P. Blanc, and M. Krisch, J. Appl. Phys. **71**, 145 (1992).

[19] D. Bellet and G. Dolino, Thin Solid Films **276**, 1 (1996).

[20] D. Buttard, D. Bellet, and G. Dolino, J. Appl. Phys. **79**, 8060 (1996); D. Bellet, S. Billat, G. Dolino, M. Ligeon, C. Meyer, and F. Muller, Solid State Commun. **86**, 51 (1993).

[21] D. Buttard, G. Dolino, Y. Campidelli, A. Halimaoui, and D. Bensahel (unpublished).

[22] D. Bellet and G. Dolino, Phys. Rev. B **50**, 17 162 (1994).

[23] G. Dolino and D. Bellet, Thin Solid Films **255**, 132 (1994).

[24] G. Bomchil, A. Halimaoui, and R. Hérino, Microelectron. Eng. **8**, 293 (1988); R. L. Smith and S. D. Collins, J. Appl. Phys. **71**, R1 (1992).

[25] M. I. J. Beale, N. G. Chew, M. J. Uren, A. G. Cullis, and J. D. Benjamin, Appl. Phys. Lett. **46**, 86 (1985).

[26] R. Hérino, G. Bomchil, K. Barla, C. Bertrand, and J. L. Ginoux, J. Electrochem. Soc. **134**, 1994 (1987).

[27] A. Loni, A. J. Simons, L. T. Canham, H. J. Philips, and L. G. Earwaker, J. Appl. Phys. **76**, 2825 (1994).

[28] H. Sugiyama and O. Nittono, J. Cryst. Growth **103**, 156 (1990).

[29] L. T. Canham and A. J. Groszek, J. Appl. Phys. **72**, 1558 (1992).

[30] A. Adamson, *Physical Chemistry of Surfaces* (Wiley, New York, 1976).

[31] G. W. Scherer, J. Am. Ceram. Soc. **69**, 473 (1986).

[32] R. S. Haines and R. McIntosh, J. Chem. Phys. **15**, 28 (1947).

[33] E. O. Wiig and A. J. Juhola, J. Am. Chem. Soc. **71**, 4 (1949); **71**, 561 (1949).

[34] C. H. Amberg and R. McIntosh, Can. J. Chem. **30**, 1012 (1952).

[35] M. J. Lakhanpal and E. A. Flood, Can. J. Chem. **35**, 887 (1957).

[36] R. Shuttleworth, Proc. R. Soc. (London) Ser. A **63**, 444 (1950).

[37] G. D. Halsey, J. Chem. Phys. **81**, 2076 (1977); Surf. Sci. **72**, 1 (1978).

[38] J. J. Magda and M. Tirrell, J. Chem. Phys. **83**, 1888 (1985).

[39] P. B. Balbuena, D. Berry, and K. E. Gubbins, J. Phys. Chem. **97**, 937 (1993).

[40] H. K. Christenson, Phys. Rev. Lett. **73**, 1821 (1994); J. Crassous, E. Charlaix, and J. L. Loubet, Europhys. Lett. **28**, 37 (1994).

[41] V. M. Nabutovskii and V. R. Belosludov, Int. J. Mod. Phys. B **3**, 171 (1989).

[42] E. Cheng and M. W. Cole, Phys. Rev. B **41**, 9650 (1990).

[43] B. K. Peterson, K. E. Gubbins, G. S. Heffelfinger, U. Marini Bettolo Marconi, and F. van Swol, J. Chem. Phys. **88**, 6487 (1988).

[44] M. Napiorkowski, W. Koch, and S. Dietrich, Phys. Rev. B **45**, 5760 (1992).

[45] I. M. Young, M. I. J. Beale, and J. D. Benjamin, Appl. Phys. Lett. **46**, 1133 (1985).

[46] H. J. Wasserman and J. S. Vermaak, Surf. Sci. **32**, 168 (1972).

[47] T. Itoh, H. Kiyama, T. Yasumatsu, H. Watanabe, and H. Hiraki, Physica B **170**, 535 (1991).

[48] D. Buttard, D. Bellet, and G. Dolino, J. Appl. Phys. **79**, 8060 (1996).

[49] H. J. McSkimin and P. Andreatch, J. Appl. Phys. **35**, 7 (1964); **35**, 2161 (1964).

[50] R. J. Jaccodine, J. Electrochem. Soc. **110**, 524 (1963).

[51] *Handbook of Chemistry and Physics*, 61st ed., edited by R. C. Weast and M. J. Astle (CRC, Boca Raton, FL, 1981).

[52] R. Defay, I. Prigogine, A. Bellemans, and D. H. Everett, *Surface Tension and Adsorption* (Longmans, Green & Co, London, 1966).

[53] J. A. Duffy, N. Wilkinson, H. M. Fretwell, M. A. Alam, and R. Evans, J. Phys. Condens. Matter **7**, L713 (1995).

[54] D. H. Bangham and R. I. Razouk, Proc. R. Soc. London Ser. A **166**, 572 (1938).

[55] D. H. Bangham and R. I. Razouk, Trans. Faraday Soc. **33**, 1459 (1937); **33**, 1463 (1937).

[56] G. E. Boyd and H. K. Livingston, J. Am. Chem. Soc. **64**, 2383 (1942).

[57] R. K. Iler, *The Chemistry of Silica* (Wiley, New York, 1979); G. Vigil, Z. Xu, S. Steinberg, and J. I. Israelachvili, J. Colloid Interf. Sci. **165**, 367 (1994).

[58] C. J. van Oss, *Interfacial Forces in Aqueous Media* (Marcel Dekker Inc., New York, 1994).

[59] R. William and A. M. Goldman, Appl. Phys. Lett. **25**, 531 (1974).

[60] C. R. Helms and E. H. Pointdexter, Rep. Prog. Phys. **57**, 791 (1994).

[61] G. Gould and E. A. Irene, J. Electrochem. Soc. **135**, 1535 (1988).

[62] D. Beaglehole and H. K. Christenson, J. Phys. Chem. **96**, 3395 (1992).

[63] W. H. Lawnick, U. D. Goepel, A. K. Klouk, and G. H. Findenegg, Langmuir **11**, 3075 (1995).

[64] P. Dumas, Y. J. Chabal, and P. Jacob, Surf. Sci. **269/270**, 867 (1992).

[65] J. Visser, Adv. Colloid Interf. Sci. **3**, 331 (1972); I. M. Tidswell, T. A. Rabedeau, P. S. Pershan, J. P. Folkers, M. V. Baker, and G. M. Whitesides, Phys. Rev. B **44**, 10 869 (1991).

[66] G. J. Pietsch, G. S. Higashi, and Y. J. Chabal, Appl. Phys. Lett. **63**, 1264 (1994).

[67] A. Halimaoui, Appl. Phys. Lett. **63**, 1264 (1993).

[68] A. Marmur, Adv. Colloid Interf. Sci. **50**, 121 (1994).

[69] P. C. Pearson, J. M. Macaulay, and S. M. Prokes, J. Electrochem. Soc. **139**, 3373 (1992).

[70] J. Tse and A. W. Adamson, J. Colloid Interf. Sci. **72**, 515 (1979).

[71] M. E. Schrader and G. H. Weiss, J. Phys. Chem. **91**, 353 (1987).

[72] F. M. Fahran, E. A. Flood, M. L. Lakhanpal, and B. Evans, Can. J. Chem. **45**, 589 (1967).

[73] M. Strezelczyk, P. Müller-Buschbaum, M. Tolan, and W. Press, Phys. Rev. B **52**, 1689 (1995).

[74] U. Grüning and A Yelon, Thin Solid Films **255**, 135 (1995).

[75] O. Kadlec and M. M. Dubinin, J. Colloid Interf. Sci. **31**, 479 (1969); J. C. P. Broeckhoff and W. P. van Beek, J. Chem. Soc. Trans. Faraday Soc. I **75**, 42 (1979).

[76] A. G. Cullis and L. T. Canham, Nature **353**, 335 (1991); E. Takasuka and K. Kamei, Appl. Phys. Lett. **65**, 484 (1994).

[77] S. Schuppler, S. L. Friedman, M. A. Marcus, D. L. Adler, Y. H. Xie, F. M. Ross, Y. J. Chabal, T. D. Harris, L. E. Brus, W. L. Brown, E. E. Chaban, P. F. Szajowski, S. B. Christman, and P. H. Citrin, Phys. Rev. B **52**, 4910 (1995).

[78] (a) A. G. Foster, Trans. Faraday Soc. **28**, 645 (1932); (b) J. Chem. Soc. 1806 (1952).

[79] (a) H. Cohan, J. Am. Chem. Soc. **60**, 433 (1938); (b) **66**, 98 (1944).

[80] D. H. Everett, in *Solid Gas Interfaces*, edited by E. A. Flood (Marcel Dekker, New York, 1967), Vol. 2, p. 1055.

[81] G. Mason, Proc. R. Soc. London **415**, 453 (1988).

[82] P. C. Ball and R. Evans, Europhys. Lett. **4**, 715 (1987).

[83] J. C. P. Broekhoff and J. H. de Boer, J. Catal. **9**, 8 (1967); W. F. Saam and M. W. Cole, Phys. Rev. B **11**, 1086 (1975).

[84] U. Marini Bettolo Marconi and F. Van Swol, Phys. Rev. A **39**, 4109 (1989).

[85] V. Vezin, P. Goudeau, A. Naudon, A. Halimaoui, and G. Bomchil, Appl. Phys. Lett. **60**, 2625 (1992).

[86] J. R. Dacey and M. J. B. Evans, Carbon **9**, 579 (1971).

[87] R. Evans and U. Marini Bettolo Marconi, J. Chem. Phys. **86**, 2376 (1986).

[88] L. J. Gibson and M. F. Ashby, *Cellular Solids: Structure and Properties* (Pergamon, London, 1988).

[89] J. R. M. Da Fonseca, J. M. Saurel, A. Foucaran, J. Camassel, E. Massone, T. Taliercio, and Y. Boumaiza, J. Mater. Sci. **30**, 35 (1995).

[90] D. Bellet, P. Lamagnère, A. Vincent, and Y. Bréchet, J. Appl. Phys. **80**, 3772 (1996).

[91] L. T. Canham, A. G. Cullis, C. Pickering, O. D. Dosser, T. I. Cox, and T. P. Lynch, Nature **368**, 133 (1994).

[92] O. Belmont, C. Faivre, D. Bellet, and Y. Bréchet, Thin Solid Films **276**, 219 (1996); O. Belmont, D. Bellet, and Y. Bréchet, J. Appl. Phys. **79**, 7586 (1996).

[93] G. Amato and N. Brunetto, Mater. Lett. **26**, 295 (1996).